Computers, Materials & Continua CMC, vol.62, no.1, pp.79-97, 2020

Multi-Scale Analysis of Fretting Fatigue in Heterogeneous Materials Using Computational Homogenization

Dimitra Papagianni[1, 2] and Magd Abdel Wahab[3, 4, *]

Abstract: This paper deals with modeling of the phenomenon of fretting fatigue in heterogeneous materials using the multi-scale computational homogenization technique and finite element analysis (FEA). The heterogeneous material for the specimens consists of a single hole model (25% void/cell, 16% void/cell and 10% void/cell) and a four-hole model (25% void/cell). Using a representative volume element (RVE), we try to produce the equivalent homogenized properties and work on a homogeneous specimen for the study of fretting fatigue. Next, the fretting fatigue contact problem is performed for 3 new cases of models that consist of a homogeneous and a heterogeneous part (single hole cell) in the contact area. The aim is to analyze the normal and shear stresses of these models and compare them with the results of the corresponding heterogeneous models based on the Direct Numerical Simulation (DNS) method. Finally, by comparing the computational time and % deviations, we draw conclusions about the reliability and effectiveness of the proposed method.

Keywords: Fretting fatigue, multi-scale analysis, computational homogenization, heterogeneous materials, stress analysis, finite element analysis.

1 Introduction

Fretting fatigue occurs due to the periodic contact of two surfaces. We can consider it as fatigue resulting of micro-friction. Essentially, it occurs due to the oscillatory tangential relative movement of two contact surfaces along with an axial load. Its applications seem to be in all types of situations involving machines under the condition of fretting [Matikas and Nicolaou (2009); Wittkowsky, Birch, Dominguez et al. (1999)]. Areas under this kind of friction are sensitive to fatigue cracking and consequently to the reduction of lifetime of the structure. This is a complex phenomenon though interesting to study and understand because plenty of costly and dangerous situations can be avoided in industries like civil and aerospace engineering. Due to its severity, this phenomenon has attracted the interest of many researchers both in experimental and theoretical approaches and it is

[1] Department of Materials Science and Engineering, University of Ioannina, Ioannina, Greece.

[2] Soete Laboratory, Faculty of Engineering and Architecture, Ghent University, Technologiepark Zwijnaarde 903, Zwijnaarde B-9052, Belgium.

[3] Division of Computational Mechanics, Ton Duc Thang University, Ho Chi Minh City, Vietnam.

[4] Faculty of Civil Engineering, Ton Duc Thang University, Ho Chi Minh City, Vietnam.

[*] Corresponding Author: Magd Abdel Wahab. Email: magd.abdelwahab@tdtu.edu.vn.

being systematically investigated from the 1940's. In 1953, progress was made and fretting along with fatigue was identified as a more severe condition for mechanical components affecting the material's properties. Later, from 1960 many researchers started to shed light on effects like crack initiation and the factors that affects it and further experiments were conducted and it was concluded that other factors like contact area and size were significant for fretting fatigue. Many other attempts of more advanced modeling have been made focusing on stress concentration effects and micro crack initiation mechanisms [Ciavarella and Demelio (2001)]. Recently, many research articles have been published to study fretting fatigue, including stress analysis, crack initiation and crack propagation [Bhatti and Wahab (2018); Kosec, Slak, Depolli et al. (2019)].

Sometimes, engineers intentionally design materials using detachments of inclusions inside the materials because this increases its ductility. This is preferable to generating surface tensions that are generally considered to be more catastrophic for the material's lifecycle. In recent years, research for heterogeneous materials has been made and composites and metal alloys have taken the place of traditional materials with the purpose of improving its mechanical properties, reducing cost, etc. A very effective and practical way to study this kind of problems is through numerical analysis and finite element packages. Therefore, when it comes to fretting fatigue, in previous studies, stress behavior of heterogeneous specimens problems has been analyzed using Direct Numerical Simulation (DNS) effectively, giving valuable information [Pereira, Bordas, Tomar et al. (2016)]. Another very important factor for simulations is the computational cost. Heterogeneous materials, especially those that have periodicity in their structure, can be simulated by the technique of computational homogenization.

Numerical homogenization techniques are used to derive the effective properties of a material working on a Representative Volume Element (RVE) of the heterogeneous medium. This can be achieved with several methods using different homogenization techniques for periodic or random microstructures [He, Wang and Pindera (2019); Gao, van Dommelen and Geers (2017)]. The unit cell method is one of those numerical approximations that give us the materials homogenized properties when the RVE is subjected to certain boundary conditions and then the average values of stresses and strains are used to obtain the effective properties. The basic concept of this idea is to find the globally homogeneous medium equivalent to the original heterogeneous model [Bergera, Karia, Gabberta et al. (2005); Moreno, Tita and Marques (2009)]. In this paper, fretting fatigue stress behavior of homogeneous models with effective properties that have been calculated through the computational homogenization technique is presented. A unit cell method of periodic heterogeneous structures is considered using the finite element method. Models with homogeneous and heterogeneous parts concerning their properties have been constructed, and their results are compared with the corresponding cases of heterogeneous Fretting Fatigue models calculated by direct numerical simulation (DNS) method. Finally, we assess the agreement of the results and see if the computational cost has been reduced while maintaining credible results.

2 Analytical and numerical homogenization methods

2.1 RVE-Theoretical background

Scale homogenization is a mathematical technique, which was developed by mathematicians in the 70's. Homogenization theory connects the macroscopic and microscopic properties of heterogeneous materials with relationships. The multi scale approach gives us the details of these relationships and the key is to determine the periodic object in a manner that the geometrical and physical characteristics are included. A periodic unit cell or RVE will contain all the necessary information, needed to compute the elastic, thermal, magnetic and electric properties. In the case that a phase-1 is scattered in phase-2 there is heterogeneity (Fig. 1). For example, in composite materials with reinforced fibers, this dimension is the average of the distance between the parallel fibers. In addition, there is also a scale δ in which properties of the material can be approached satisfactorily, in the sense of the average value. This means that if the properties of the material are studied in segments of the material size δ, their measured values should be independent of position of the segment into the material. In this sense, the material can be seen as homogeneous with properties that have been determined at its level scale δ. In the case where such a scale can exist, (i.e., a scale between the scale of the components and the scale of the composite material), we say the material can be homogenized. The idea of converting a heterogeneous material into an equivalent (in some way) "seemingly" homogeneous is called homogenization. Many scientists have developed several approaches to solve scale transition problems. Analytical approaches have been reported like the rule of mixtures in which the only defining parameters are these of the elastic properties and the volume fraction of every phase. As a result, the new effective properties of the composite can be calculated. In 1960's, the variational bounding technique of linear elasticity was introduced. In these models, an RVE is selected and boundary conditions are imposed. A big step for employing the elasticity equations along with energy methods to develop equations for inclusion problems was taken. In 1973, Mori and Tanaka studied the behavior of the particle size and concluded that this has an important effect on the behavior of the composite material, namely hardening for small particles and softening for large particles [Tan, Huang, Liu et al. (2005)].

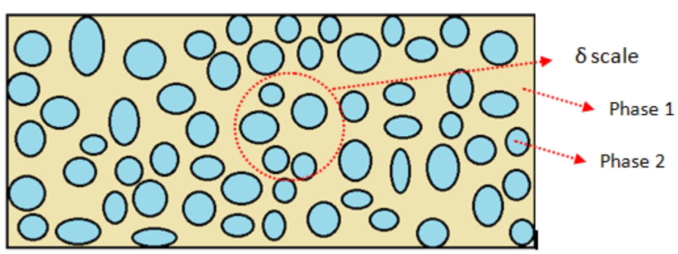

Figure 1: Homogenization of a heterogeneous material

2.2 Unit cell method

Even though analytical approaches contributed in these kinds of problems, numerical models seem to have a very good approach for homogenization techniques as by modeling along with finite element method. We can handle complex geometries, several material properties, size in micro and nano scales and even different phases. Micromechanical method is one of them and provides the overall behavior of the composite (matrix with second phase like fibers or inclusions) using a unit cell or RVE. The heterogeneous structure is replaced by an equal homogeneous medium with the global properties of the composite. This technique is useful not only for the computational cost reduction but also for the successful study of many mechanical effects like damage initiation and propagation. After choosing the RVE, appropriate boundary conditions must be imposed and after post processing, we have all the results we need to proceed and calculate the effective properties using the following equations:

$$\overline{S_{ij}} = \frac{1}{V}\int_V S_{ij}dV \tag{1}$$

$$\overline{T_{ij}} = \frac{1}{V}\int_V T_{ij}dV \tag{2}$$

Practically, we multiply the stresses or strains that act on the nodes of each element with the volume of each element. Then, we sum the resulting product and we divide it by the volume of the RVE. This is how we get the average stress and strain values. Finally, we divide the average stress value with the strain and as results we get the effective stiffness constants C_{ij}^{eff} which we use to calculate the global properties, Young Modulus E^* *and* Poisson's ratio v^* of the composite.

3 Numerical models

3.1 Direct numerical simulation method

Direct numerical Simulation (DNS) method has been used for solid mechanics problems for heterogeneous materials even though it has been introduced in modeling of fluid mechanics. DNS is a numerical approach that gives reliable results when the mathematical problem and the equations that govern it are solved. The results of this work are compared with those of DNS case studied for the first time the fretting fatigue stress behavior of heterogeneous materials [Kumar, Biswas, Poh et al. (2017)]. A fretting fatigue specimen was constructed with circular micro-voids having dimensions 2 mm×1 mm i.e., the specimen contains 100 cells in total with various percentage of voids from 1.5%-25% and applied eight different test conditions. Based on Kumar et al. [Kumar, Biswas, Poh et al. (2017)], we continue this work on the fretting fatigue model case with 25%, 16% and 10% micro-voids. These heterogeneous specimens are replaced by a homogeneous one through an analysis of periodic RVE or unit cell.

3.2 RVE for heterogeneous material

After creating a heterogeneous model, see Fig. 2. We build and work in a new cell model, which is a part of the heterogeneous specimen. Due to the periodicity of the structure it is easy to choose the representative volume element (RVE). We want to predict the effective properties of the cell with 25%, 16% and 10% void ratios. Similarly, with the previous case, this is a 2-D model with dimensions: 2 mm×1 mm and radius of hole: 0.4

mm, 0.3 mm and 0.2 mm. The goal here is to calculate the effective properties of the unit cell and use it as the input material properties in macro-scale model as they will be the equivalent properties of the heterogeneous case. The computational homogenization technique is implemented through the easy periodic boundary conditions plug-in in ABAQUS, which is explained in Section 3.2 [Omairey, Dunning and Sriramula (2019)]. After the procedure is finished we get the new properties, which are Young's modulus E^*=35.4 GPa and Poisson's ratio v^*=0.26 for 0.4 mm radius models, E^*=55.6 GPa, v^*=0.3 for 0.3 mm radius models and E^*=61.8 GPa, v^*=0.32 for 0.2 mm radius models.

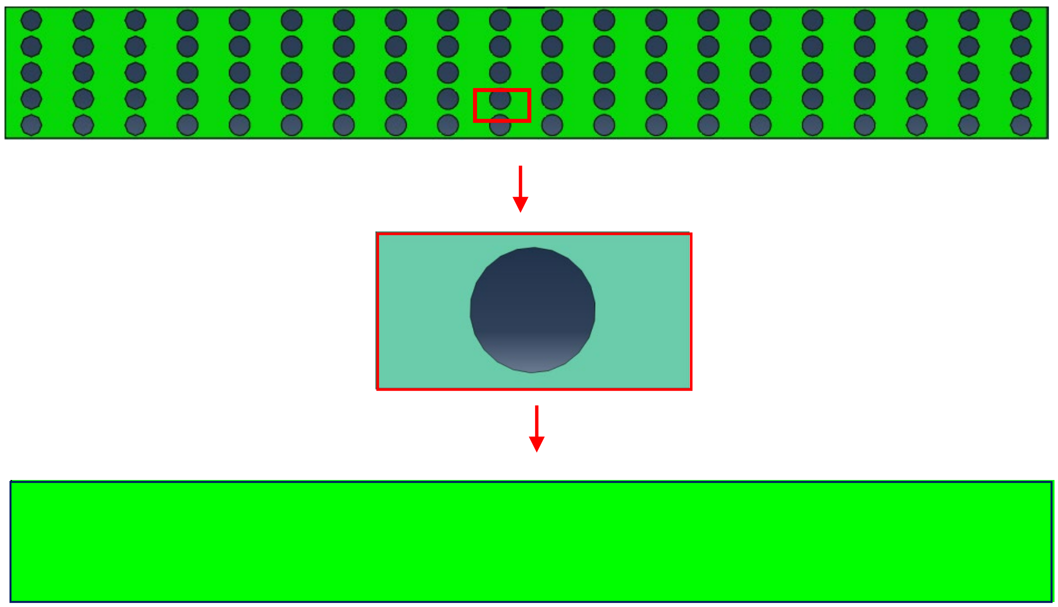

Figure 2: Choosing the RVE

3.3 Computational homogenization process

In this step, we want to convert the heterogeneous specimen to an equal homogeneous specimen considering its mechanical properties. We are working on a 2-D RVE as it is chosen in a way that captures the major features of the underlying microstructure. We are using the finite element package ABAQUS and a special plug-in created in Ref. [Omairey, Dunning and Sriramula (2019)], which uses an automatic operation to calculate the effective properties. Specifically, the steps followed are:

i) Definition of a Reference Point=dummy node, outside the geometry

ii) Creation of 2 sets of opposite nodes (four edges of RVE)

iii) Tie the opposite node sets together through constraint equations by applying displacements on the Reference point

iv) Calculation of the effective properties through the average values of stresses and strains in every node [Wu, Owino, Al-Ostaz et al. (2014)].

3.4 Fretting fatigue macro model

The fretting fatigue models were built and solved using the finite element package ABAQUS 6.14. The specifications of the machine used to solve this simulation had Processor: Dubbele Intel Xeon Gold 6130 2, 1 GHz, 3.7 GHz Turbo, 16C, 10,4 GT/s 2 UPI, 22 MB cache, HT (125 W) DDR4-2666, RAM: 128 GB(16×8 GB) 2666 MHz DDR4 RDIMM ECC, VIDEO: NVIDIA® Quadro® P2000, 5 GB, 4 DP (7920 rack), HD: RAID 5-5×600 GB 2.5''SAS 12 (15000 rpm). The fretting fatigue models that describe the contact problem consist of a pad and a heterogeneous specimen. The dimensions are taken from Kumar et al. [Kumar, Biswas, Poh et al. (2017)]. About the specimen, the length is equal to 40 mm, the width is equal to 5 mm, the thickness is 4 mm and the radius of the holes is 0.4 mm and 0.3 mm. Every cell is 2 mm×1 mm with a single-hole with the above mentioned radius leading to a 25% of void for the 0.4 mm hole and 16% of void for the 0.3 mm hole. The pad's dimensions are: length: 10 mm, width: 10 mm and radius of contact surface: 50 mm. Both the pad and the specimen are made from Aluminum Alloy AL7075-T6, with Young's Modulus E=74.1 GPa and Poisson's ratio ν=0.33. As for the element a 2-D four node plane strain was used for both pad and specimen. The contact area was meshed with a 5 μm×5 μm element that is a decent size to capture this complex contact phenomenon. For the contact simulation we had to include the Lagrange multiplier friction to define the contact behavior of the contact region with μ=0.65.

The loading condition used to simulate the effect of fretting fatigue is taken from the experimental data in Talemi et al. [Talemi, Wahab, De Pauw et al. (2014)]. Stress analysis was performed applying FF2 loading case [Kumar, Biswas, Poh et al. (2017)] with a normal stress F=543 N in Y direction on top surface of the pad in a reference point. This load remains constant till the end of the cycle. Oscillatory axial and reaction stresses in the right and left edges of the specimen are applied reflecting the fretting cycle. The bottom edge of the specimen is restricted in the Y direction U_y=0 and the right and left edges of the pad are restricted in the X direction U_x=0. In addition, MPC tie constraint was used to ensure no rotation will appear due to the Load in Y direction (normal stress). Fig. 3 shows the heterogeneous model using DNS.

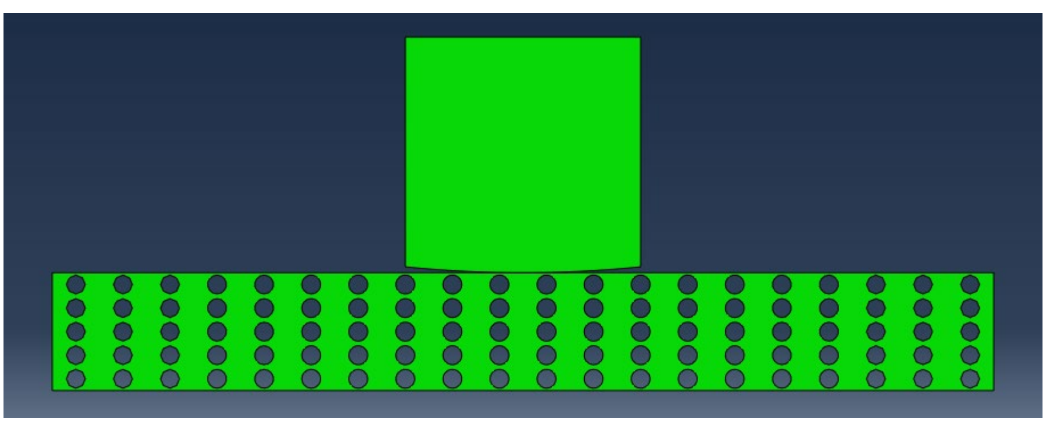

Figure 3: Heterogeneous specimen using DNS 1-hole (25% void)

The homogeneous model in Fig. 4 represents the equally homogeneous model, where the mechanical properties applied are those calculated by multiscale homogenization method. From now on, we will call this model case 1: full homogenization. This model is imposed to FF2 loading case and normal and shear stress distributions along the contact area are constructed and will be compared with DNS 1 - hole case.

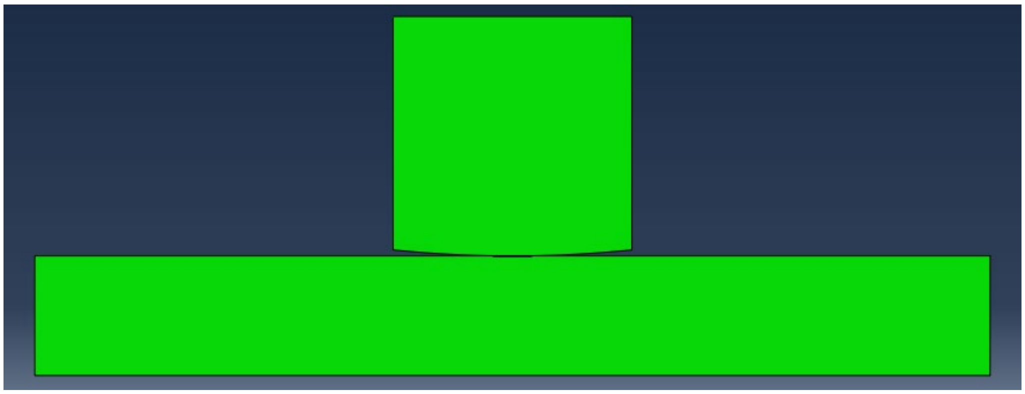

Figure 4: Case 1: full homogenization

The fretting fatigue contact problem is performed for the two extra cases that their specimens consist of a homogeneous and a heterogeneous part (single- and four-hole cell) in the contact area, cases 2 and 5, as shown in Fig. 5(a) and Fig. 5(d), respectively. These two models are constructed with the same procedure as mentioned before. The reason why we create these two models is to simulate better the contact problem concerning the heterogeneous specimen. Thus, as shown in Fig. 5(a) and Fig. 5(d) in both cases the pad is in contact with 2 cells which have a single hole with radius 0.4 mm and four holes with radius 0.2 mm leading to a 25% void (heterogeneous part). For the homogeneous part, we use the mechanical properties that we calculated earlier with the computational homogenization technique using RVE. Then, we perform the same simulation for the two models and we make graphs for the normal and shear stress distribution along the contact area**.** This procedure is repeated for both 0.3 mm radius -16% void/cell model and 0.2 mm radius -10% void/cell model.

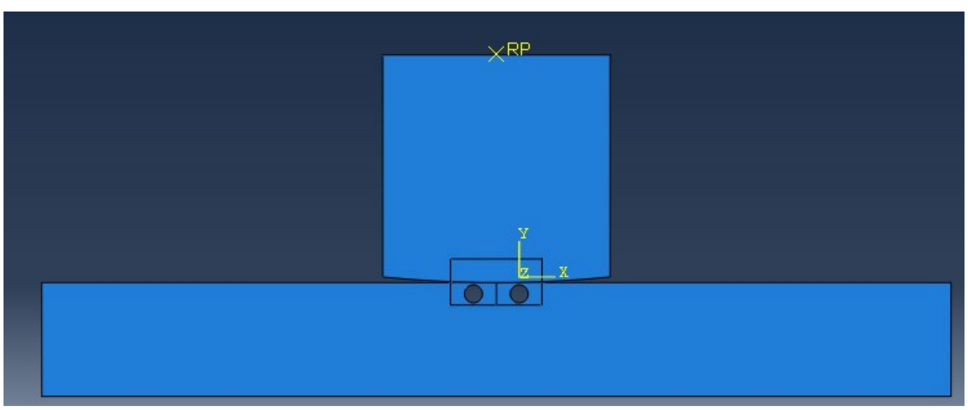

Figure 5(a): Case 2: partial homogenization 2-cell 1-hole

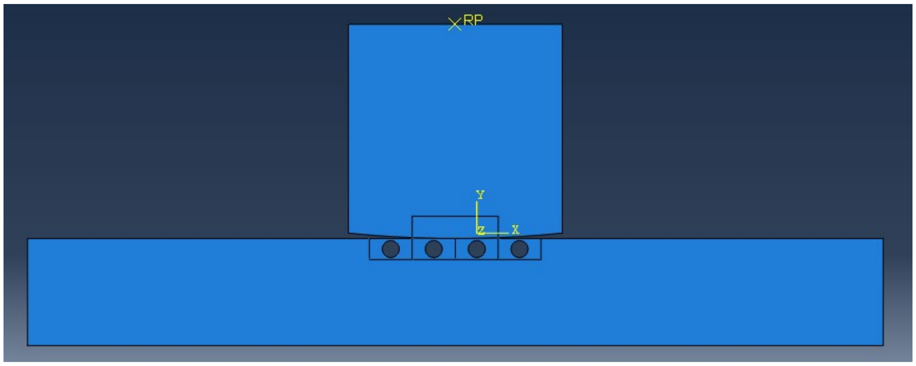

Figure 5(b): Case 3: partial homogenization 4-cell 1-hole

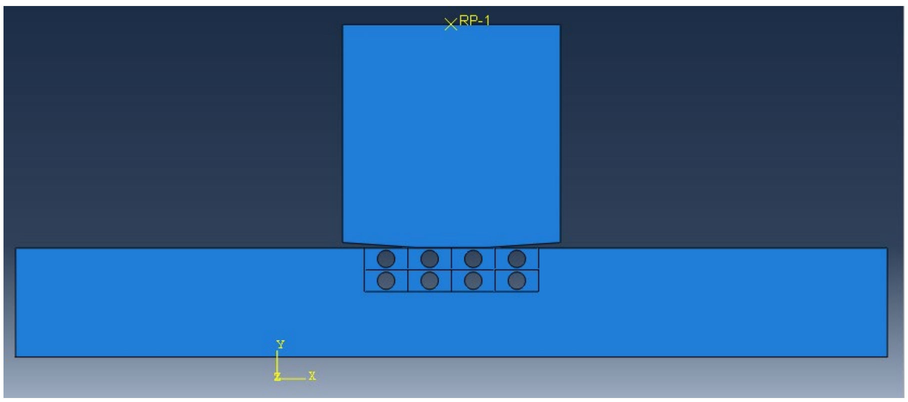

Figure 5(c): Case 4: partial homogenization 8-cell 1-hole

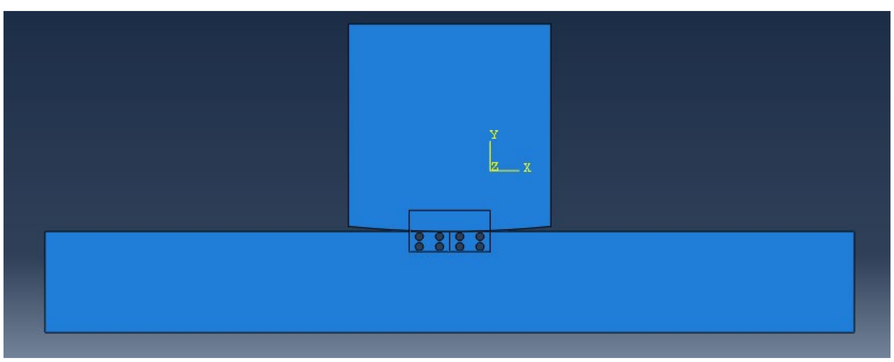

Figure 5(d): Case 5: partial homogenization 2-cell 4-hole

We want to further examine whether the fretting fatigue phenomenon can be better modeled and give us even better results while maintaining the computational time less than that of the DNS cases. That's why we constructed two more models with 4 and 8 cells that we call case 3: partial homogenization 4-cell 1-hole (Fig. 5(b)) and case 4: partial homogenization 8-cell 1-hole (Fig. 5(c)). These two models are imposed to FF2 loading case as well and normal and shear stress distributions along the contact area are constructed and compared with DNS 1-hole case for 0.4 mm radius -25% void/cell, 0.3 mm radius -16% void/cell and 0.2 mm radius -10% void/cell.

4. Results and discussion

4.1 Case 1: full homogenization with DNS 1- hole

In order to investigate if the homogenization method is reliable and valid, we constructed graphs of normal and shear stress distribution along the contact interface. At first, we created graphs, normal and shear stress distributions along the contact area for case 1 with the new effective properties and we compared them with the corresponding graphs of the DNS (single hole) case. From Fig. 6 and Fig. 7, as it was expected the results for case 1 compared to DNS-1 hole case are not close. This is because the fact that the contact stress is affected by the precise of holes, which are not explicitly modelled in the macro-model.

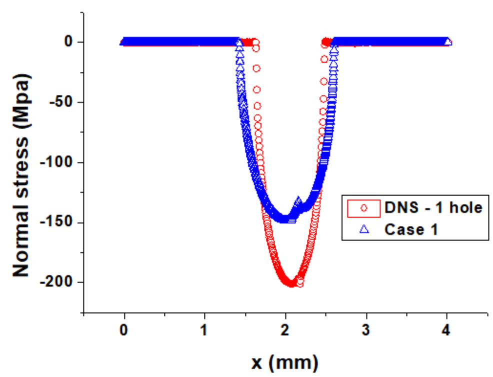

Figure 6: Normal stress distribution along contact area for DNS 1-hole and case 1 (0.4 mm radius)

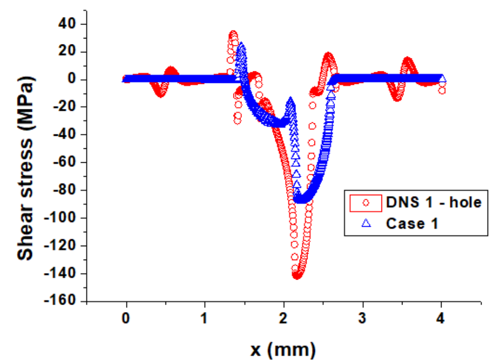

Figure 7: Shear stress distribution along contact area for DNS 1-hole and case 1 (0.4 mm radius)

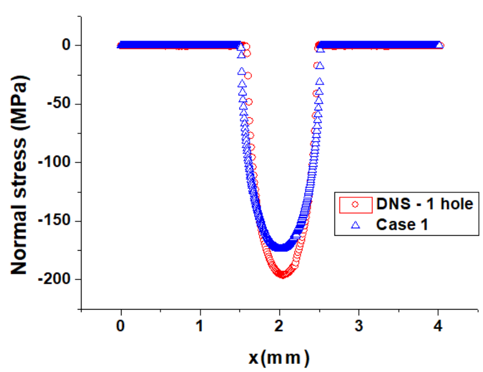

Figure 8: Normal stress distribution along contact area for DNS 1-hole and case 1 (0.3 mm radius)

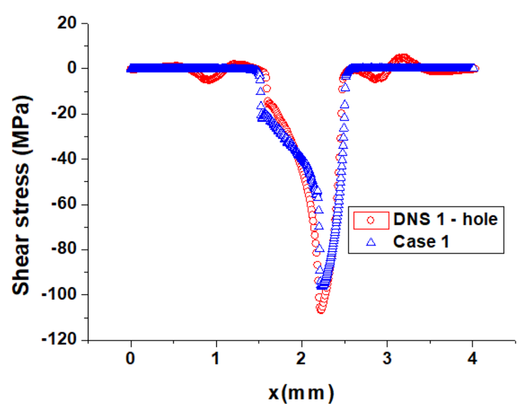

Figure 9: Shear stress distribution along contact area for DNS 1-hole and case 1 (0.3 mm radius)

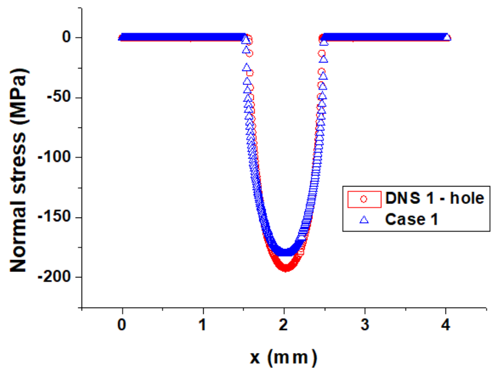

Figure 10: Normal stress distribution along contact area for DNS 1-hole and case 1 (0.2 mm radius)

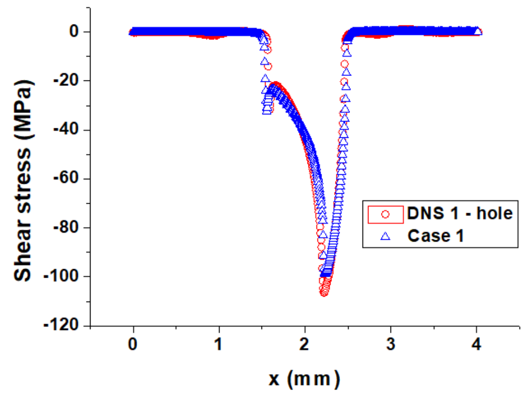

Figure 11: Shear stress distribution along contact area for DNS 1-hole and case 1 (0.2 mm radius)

We can see in Fig. 6 and Fig. 7 that the results of case 1 (0.4 mm radius of hole) for both normal and shear stress distributions are not in agreement with those of the DNS single hole case. The next step to improve the results is to better express the interface problem and at the same time keep the computational time low. This will be achieved by maintaining the heterogeneity at the contact area. In Figs. 8 and 9 the plots of case 1 (0.3 mm radius of hole) have been improved and the trends seem to fit more than the 0.4 mm hole case. In Fig. 10 and Fig. 11 for case 1 (0.2 mm radius of hole) we notice significant improvement for both cases since the trends fit better than the two other cases and the deviations are very small. This is reasonable since the radius of the hole is smaller and the homogeneous properties are closer to the original material values.

4.2 Cases 2, 3 and 4: partial homogenization

4.2.1 One hole per cell-0.4 mm radius (25% void/cell)

As mentioned in the previous section, we need to introduce the heterogeneity into our problem to better approach it. In Fig. 5**,** we see the three models we constructed with 2 cells, 4 cells and 8 cells in the contact area. In order to come to a conclusion about the effectiveness of the method we used, we need to check how the results are improved by going from case 2 to 3 and 4 since the increase in holes better reflects the problem of heterogeneity, We also want to look at the influence of the radius of the holes. All cases are compared with the corresponding DNS cases. Our goal is to look at which of these models gives the best results through the graphs presented.

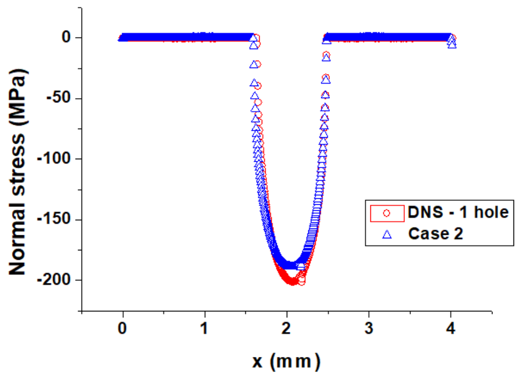

Figure 12: Normal stress distribution along contact area for DNS 1-hole and case 2 (0.4 mm radius)

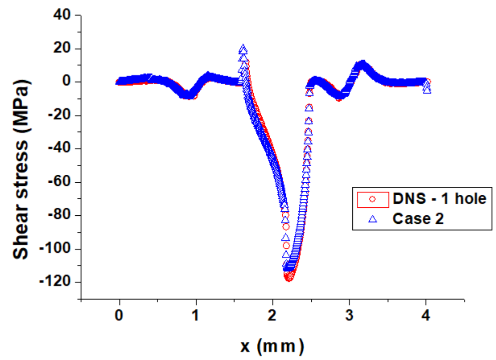

Figure 13: Shear stress distribution along contact area for DNS 1-hole and case 2 (0.4 mm radius)

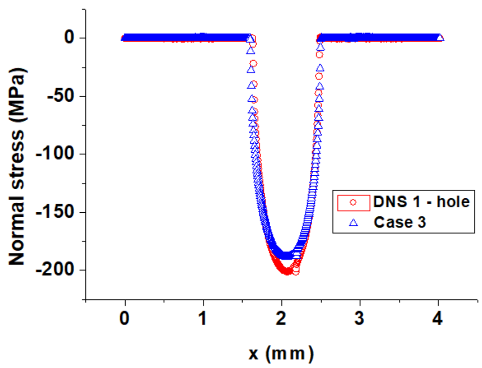

Figure 14: Normal stress distribution along contact area for DNS 1-hole and case 3 (0.4 mm radius)

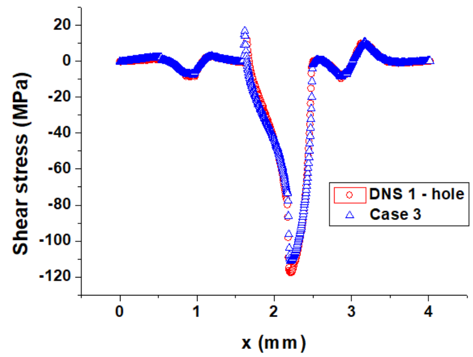

Figure 15: Shear stress distribution along contact area for DNS 1-hole and case 3 (0.4 mm radius)

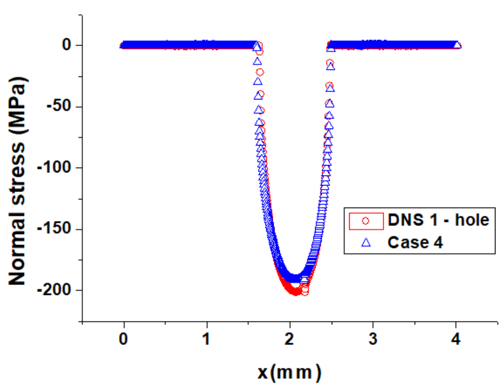

Figure 16: Normal stress distribution along contact area for DNS 1-hole and case 4 (0.4 mm radius)

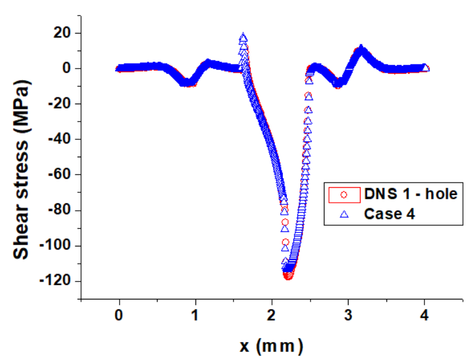

Figure 17: Shear stress distribution along contact area for DNS 1-hole and case 4 (0.4 mm radius)

Comparing case 2 and DNS 1-hole cases, Fig. 12 and Fig. 13, we observe that the results are close although in the DNS case both normal and shear stress values are higher than case 2. It can be considered that this is expected since the homogenization method is an approximate solution. Despite this assumption, we constructed a model with 4 cells in contact area and created graphs. Only by looking the trends, we do not observe any difference between Case 2 and 3 comparing with the DNS case Fig. 14 and Fig. 15. Again, differences are observed in the highest values in normal stresses. Moving to case 4 model's results both normal and shear stress distributions has shown very small improvement comparing with case 3, Fig. 16 and Fig. 17. It becomes obvious that it is necessary to examine through percentages the difference between cases.

4.2.2 One hole per cell-0.3 mm radius (16% void/cell)

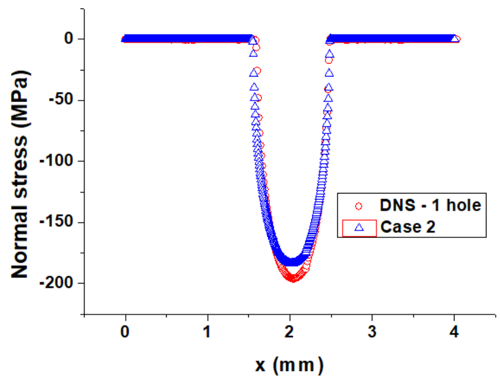

Figure 18: Normal stress distribution along contact area for DNS 1-hole and case 2 (0.3 mm radius)

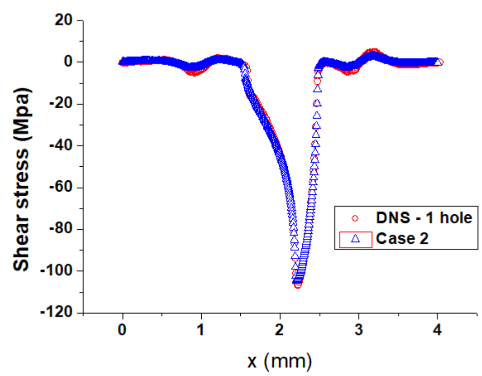

Figure 19: Shear stress distribution along contact area for DNS 1-hole and case 2 (0.3 mm radius)

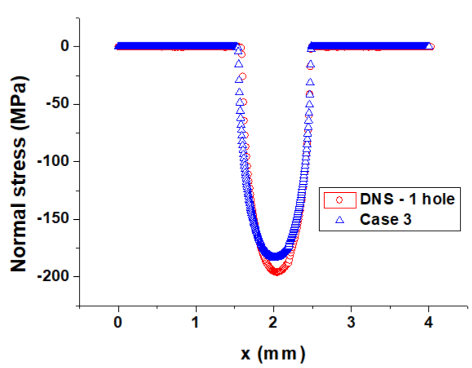

Figure 20: Normal stress distribution along contact area for DNS 1-hole and case 3 (0.3 mm radius)

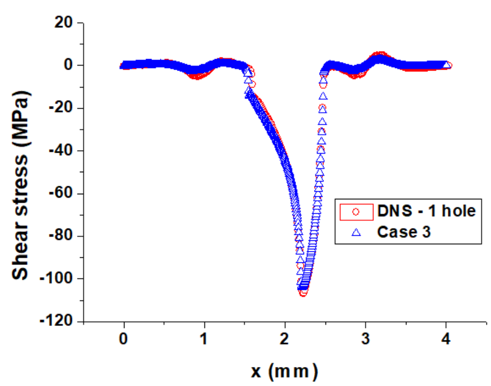

Figure 21: Shear stress distribution along contact area for DNS 1-hole and case 3 (0.3 mm radius)

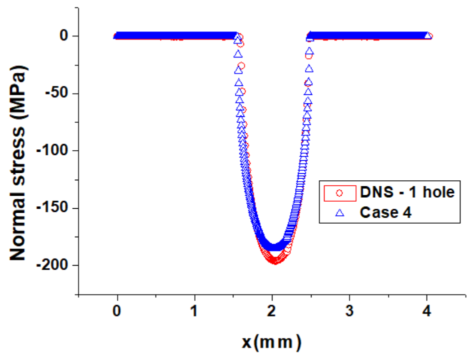

Figure 22: Normal stress distribution along contact area for DNS 1-hole and case 4 (0.3 mm radius)

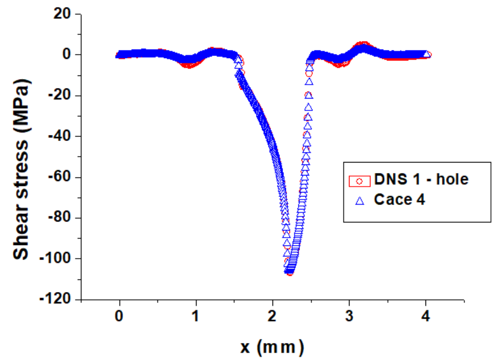

Figure 23: Shear stress distribution along contact area for DNS 1-hole and case 4 (0.3 mm radius)

4.2.3 One hole per cell-0.2 mm radius

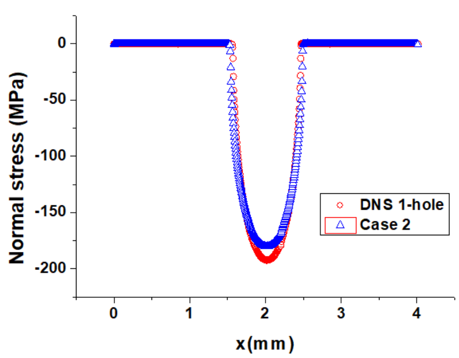

Figure 24: Normal stress distribution along contact area for DNS 1-hole and case 2 (0.2 mm radius)

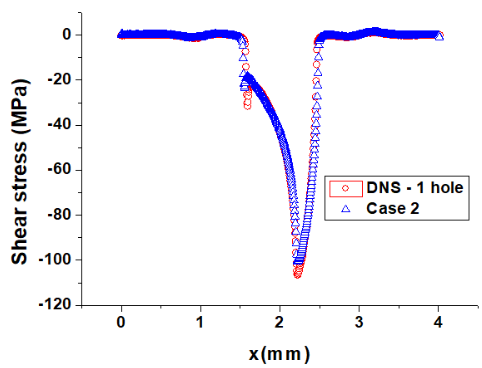

Figure 25: Shear stress distribution along contact area for DNS 1-hole and case 2 (0.2 mm radius)

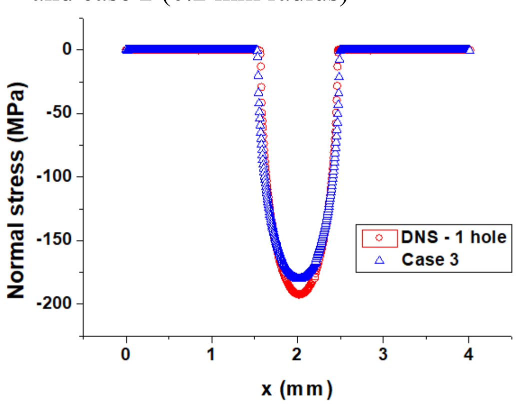

Figure 26: Normal stress distribution along contact area for DNS 1-hole and case 3 (0.2 mm radius)

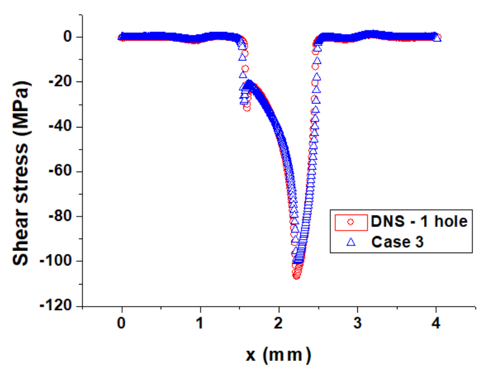

Figure 27: Shear stress distribution along contact area for DNS 1-hole and case 3 (0.2 mm radius)

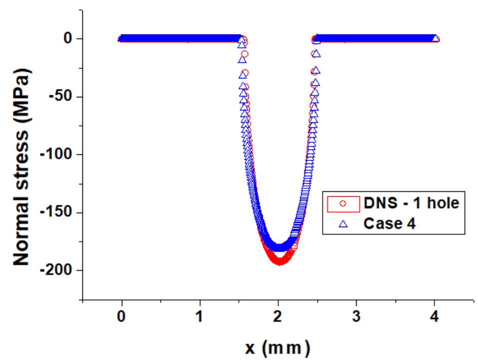

Figure 28: Normal stress distribution along contact area for DNS 1-hole and case 4 (0.2 mm radius)

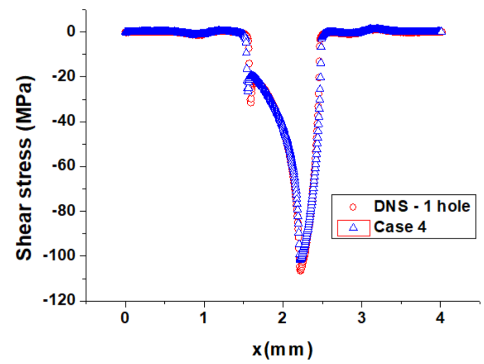

Figure 29: Shear stress distribution along contact area for DNS 1-hole and case 4 (0.2 mm radius)

Similarly, comparing normal and shear stress distributions of case 2, 3 and 4 for the 0.2 mm radius with DNS 1-hole cases, Figs. 24 to 29 with the DNS case, again, we do not notice significant differences and we need to look at the percentage difference.

4.3 Case 5: partial homogenization

4.3.1 Four holes per cell

Comparing case 5 and DNS 4-hole cases we observe that the results are in very good agreement and small deviations are noticed in the shear stress distribution, Fig. 30 and Fig. 31. We can observe that between the single (cases 2,3 and 4)-0, 4 mm radius and four (case 5) holes/ cell cases -0,2 mm radius the values of normal and shear gradients are different even though the void /cell in both cases is 25%. Particularly, the maximum normal stress value in single hole case is around 190 MPa while in 4-hole case around 240 MPa. In a related way, the shear stresses are 120 MPa and 140 MPa. It seems like the position, the geometry and the number of holes plays an important role in stress distribution and the load that the specimen can bear in fretting fatigue problems.

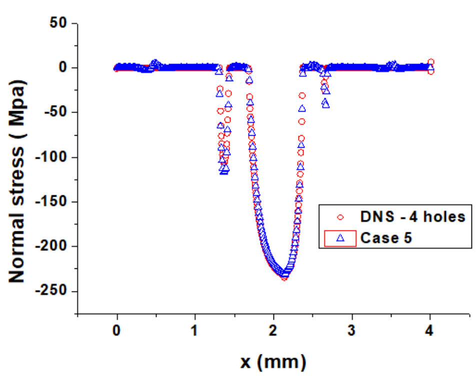

Figure 30: Normal stress distribution along contact area for DNS 4-hole and case 5 (0.2 mm radius)

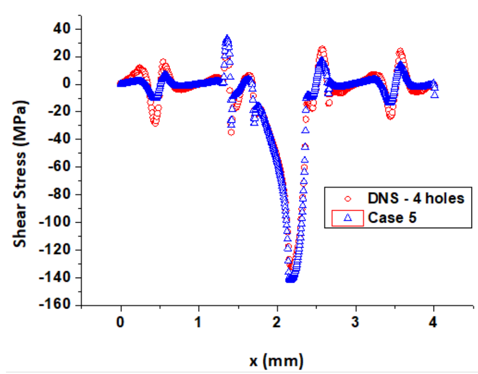

Figure 31: Shear stress distribution along contact area for DNS 4-hole and case 5 (0.2 mm radius)

4.4 Comparison of computational time and element size of all cases

Tabs. 1, 2 and 3 present the computational time and the element size in the interface for each case so that we can safely draw conclusions about the results and the effectiveness of the homogenization method. In order to better interpret our results, in Tabs. 4, 5 and 6 present the error [%] for cases 2, 3 and 4 for models with 25%, 16% and 10% void in relation to the DNS 1-hole case for normal and shear stress distributions. This was necessary as the graphs for cases 2, 3 and 4 are very close to each other and we cannot distinguish any differences so the conclusions will be revealed considering the errors between the cases. It is obvious that maintaining the same element size in every case, the computational cost of multiscale cases is reduced for cases 1, 2 and 3 and increased in cases 4 and 5 compared to the DNS cases. Particularly, case 1 has the lowest computational time but the results are not in agreement with the DNS 1-hole case except for the 0.2 mm radius of hole case 1 that has the closest trends and the % error is 6.5%. In Case 2 the results show good improvement with 2 times lower computational cost than that of DNS 1-hole case. Case 3 has almost the same behavior as case 2 but with higher computing time still less than the DNS cases. Case 4 has given the most reliable results however with computational cost 1-2 minutes more than the DNS 1-hole case still having an error. As for case 5 the CPU time was double than the DNS 4-hole case with accurate results but it was generally the most time consuming case.

Table 1: CPU time and element size of interface per case for 25% void/cell cases

Case	Total CPU time (min)	Element size-interface (μm)	Radius of hole (mm)
Case 1	12.6	5	-
Case 2	46.8	5	0.4
Case 3	89.1	5	0.4
Case 4	103.5	5	0.4
Case 5	107.5	5	0.2
DNS - 1 hole/cell	94.8	5	0.4
DNS - 4 hole/cell	59.5	5	0.2

Table 2: CPU time and element size of interface per case for 16% void/cell cases

Case	Total CPU time (min)	Element size-interface (μm)	Radius of hole (mm)
Case 1	10.8	5	-
Case 2	43.3	5	0.3
Case 3	75.3	5	0.3
Case 4	101.5	5	0.3
DNS - 1 hole/cell	98.9	5	0.3

Table 3: CPU time and element size of interface per case for 10% void/cell cases

Case	Total CPU time (min)	Element size-interface (μm)	Radius of hole (mm)
Case 1	12.6	5	-
Case 2	61.5	5	0.2
Case 3	89.1	5	0.2
Case 4	103.2	5	0.2
DNS - 1 hole/cell	102.2	5	0.2

Table 4: Comparison of cases 2, 3, 4 and 5-25% void/cell with DNS 1-hole case and 4-hole, Error [%]

0.4 mm radius cases - Normal stress (MPa)			
		DNS cases	**Error %**
Case 1	-148.2608	-200.9530	**26.22%**
Case 2	-188.7320	-200.9530	**6.08%**
Case 3	-188,8356	-200.9530	**6.02%**
Case 4	-190.9958	-200.9530	**4.95%**
Case 5	-234.4895	-235.9315	**0.61%**
0.4 mm radius cases - Shear stress (MPa)			
		DNS cases	**Error %**
Case 1	-87.3598	-117.5974	**25.71%**
Case 2	-111.7292	-117.5974	**4.99%**
Case 3	-111.8485	-117.5974	**4.88%**
Case 4	-113.5504	-117.5974	**3.44%**
Case 5	-141.7090	-136.3876	**3.75%**

Table 5: Comparison of cases 2, 3 and 4 -16% void with DNS 1-hole case, Error [%]

0.3 mm radius cases - Normal stress (MPa)			
		DNS cases	**Error %**
Case 1	-173.7118	-195.7778	**11.27%**
Case 2	-183.4447	-195.7778	**6.29%**
Case 3	-183.5508	-195.7778	**6.24%**
Case 4	-185.9122	-195.7778	**5.03%**
0.3 mm radius cases - Shear stress (MPa)			
		DNS cases	**Error %**
Case 1	-96.5567	-106.7050	**9.51%**
Case 2	-104.5684	-106.7050	**2.00%**
Case 3	-103.8965	-106.7050	**2.63%**
Case 4	-105.8271	-106.7050	**0.82%**

Table 6: Comparison of cases 2, 3 and 4-10% void with DNS 1-hole case, Error [%]

0.2 mm radius cases - Normal stress (MPa)			
		DNS cases	**Error %**
Case 1	-180.2078	-192.2992	**6.28%**
Case 2	-180.3346	-192.2992	**6.22%**
Case 3	-180.3665	-192.2992	**6.20%**
Case 4	-181.3345	-192.2992	**5.70%**
0.2 mm radius cases - Shear stress (MPa)			
		DNS cases	**Error %**
Case 1	-98.7141	-106.4463	**7.26%**
Case 2	-100.6888	-106.4463	**5.40%**
Case 3	-101.0800	-106.4463	**5.04%**
Case 4	-101.6961	-106.4463	**4.46%**

5 Conclusions

In this article, we investigated whether the multi-scale computational homogenization method can give us reliable results with lower computational cost with regard to the phenomenon of fretting fatigue in heterogeneous specimens. For that reason, we constructed homogeneous and partially homogeneous specimens where the homogeneous properties were found using (RVE) from heterogeneous specimens with 25%, 16% and 10% void/cell.

In case 1: full homogenization-no holes for homogeneous properties extracted from 0.4 mm radius of holes the normal and shear stress distributions are not in agreement with those of the DNS case with error between them 25% and computing time 12.6 minutes. It is obvious that the heterogeneity effect should be expressed so it is necessary to look in results of cases 2, 3 and 4. In case 1 for homogeneous properties extracted from 0.3 mm radius of holes the trends have been obviously improved although there are still deviations of 10% compared to the DNS case, solved in 10.6 minutes. Lastly, in case 1 for homogeneous properties extracted from 0.2 mm radius of holes we observe the best trends and an error of 6.5% compared with the DNS case. This is expected though, since the last case of 0.2 mm radius of hole has the closest mechanical properties with the original properties. The most important observation though is that Case 1 has very close results with cases 2, 3 and 4 but with significant difference in the computing time with case 1 solved in 12.6 minutes while case 4 is solved in 103.2 minutes and the DNS case solved in 102.2 minutes.

Moving to 0.4 mm radius cases 2, 3 and 4 the % error ranges from 6.08% to 4.98% for normal stress and from 4.99 % to 3.88% for shear stress with regard to the DNS case. We also observe a big difference in computing time, case 2 is solved in 46.8 minutes while case 4 solved in 103 minutes when DNS case is solved in 94.8 minutes. As for case 5 normal stress has only 0.61% difference with DNS case and 3.75% in shear stress distribution. However, the computing time of Case 5 is almost double than the DNS case. In 0.3 mm radius cases 2, 3 and 4 the % error ranges from 6.29% to 5.03% for normal stress and 2.00% to 0.82% with computing time similar to 0.4 mm radius of hole cases.

As for the 0.2 mm radius cases 2, 3 and 4 the % error ranges from 6.22% to 5.70% for normal stress and from 5.40% to 4, 46% again with similar computational cost.

We need to point out that in all models (0.2, 0.3, 0.4) mm radius of holes as we move from case 2 to case 3 and lastly to case 4, the % error comparing with the DNS cases is decreasing. Moreover the computational time of case 4 always exceeds that of DNS case and only cases 2 and 3 have lower computing time than the DNS cases. Lastly, we should mention that moving from case 2 to case 4 the % error is decreased and this was expected since the increase of heterogeneity factor approaches and captures better the heterogeneous structures.

In conclusion multi-scale computational homogenization technique had better results when applied in the 0.2 mm model cases and it is reasonable since the homogenized properties were closer to the original materials properties. We should point out that case 1: full homogenization, no holes model, had very close results with those of case 4 but with significant decrease in computing time. In 0.3 mm and 0.4 mm models the error generally varied from 4.5 to 6.5% in comparison with the DNS cases with the exception of the 0.3 mm shear stress distributions that the error varied from 2.0 to 0.82%. In all (0.2, 0.3 and 0.4) mm models cases 2 and 3 had lower computing time than the DNS case, however case 4 had higher computing time than the DNS cases. Generally, the biggest transition to improving the results was that of cases 1 to cases 2 that is from full homogenization - holes to partial homogenization-2 cells in contact area while no considerable improvements were observed moving from cases 2 to cases 3 and lastly to cases 4. We can conclude that this method generally cannot give us reliable and trustworthy results since the error varies from 2.5% to 6.9% in normal stress cases and from 5.4% to 0.8% in shear stress and also cannot save computational cost. Finally, we suggest in future work that this problem could be investigated using the 1st order homogenization technique in order to improve the accuracy of the results.

References

Bhatti, N. A.; Abdel Wahab, M. (2018a): Fretting fatigue crack nucleation: a review. *Tribology International*, vol. 121, pp. 121-138.

Bergera, H.; Kari, S.; Gabbert, U.; Rodriguez-Ramo, R.; Guinovart, R. et al. (2005): An analytical and numerical approach for calculating effective material coefficients of piezoelectric fiber composites. *International Journal of Solids and Structures*, vol. 42, no. 21-22, pp. 5692-5714.

Ciavarella, M.; Demelio, G. (2001): A review of analytical aspects of fretting fatigue with extension to damage parameters, and application to dovetail joints. *International Journal of Solids and Structures*, vol. 8, no. 10-13, pp. 1791-1811.

Gao, K.; van Dommelen, J. A. W.; Geers, M. G. D. (2017): Investigation of the effects of the microstructure on the sound absorption performance of polymer foams using a computational homogenization approach. *European Journal of Mechanics-A/Solids*, vol. 61, pp. 330-344.

He, Z.; Wang, G.; Pindera, M. J. (2019): Multiscale homogenization and localization of materials with hierarchical porous microstructures. *Composite Structures*, vol. 222, no. 110905

Hojjati Talemi, R.; Abdel Wahab, M.; De Pauw, J.; De Baets, P. (2014): Prediction of fretting fatigue crack initiation and propagation lifetime for cylindrical contact configuration. *Tribology International*, vol. 76, pp. 73-91.

Kosec, G.; Slak, J.; Depolli, M.; Trobec, R.; Resende Pereira, K. et al. (2019): Weak and strong from meshless methods for linear elastic problem under fretting contact conditions. *Tribology International*, vol. 138, pp. 392-402.

Kumar, D.; Biswas, R.; Poh, L. H.; Abdel Wahab, M. (2017): Fretting fatigue stress analysis in heterogeneous material using direct numerical simulations in solid mechanics. *Tribology International*, vol. 109, pp. 124-132.

Matikas, T. E.; Nicolaou P. D. (2009): Prediction of contact temperature distribution during fretting fatigue in titanium alloys. *Tribology Transaction*, vol. 52, no. 3, pp. 346-353.

Moreno, M. E.; Tita, V.; Marques, F. D. (2009): Finite element analysis applied to evaluation of effective material coefficients for piezoelectric fiber composites. *Brazilian Symposium on Aerospace Eng. & Applications*.

http://citeseerx.ist.psu.edu/viewdoc/download?doi=10.1.1.540.755&rep=rep1&type=pdf.

Omairey, S. L.; Dunning, P. D.; Sriramula, S. (2019): Development of an ABAQUS plugin tool for periodic RVE homogenization. *Engineering with Computers*, vol. 35, no. 2, pp. 567-577.

Resende Pereira, K. de F.; Bordas, S.; Tomar, S.; Trobec, R.; Depolli, M. et al. (2016): On the convergence of stresses in fretting fatigue. *Materials*, vol. 9, no. 8, pp. 639.

Tan, H.; Huang, Y.; Liu, C.; Geubelle, P. (2005): The Mori-Tanaka method for composite materials with nonlinear interface debonding, *International Journal of Plasticity,* vol. 21, pp. 1890-1918.

Wittkowsky, B. U.; Birch, P. R.; Dominguez, J.; Suresh, S. (1999): An apparatus for quantitative fretting testing. *Fatigue & Fracture of Engineering Materials & Structures*, vol. 22, no. 4, pp. 307-320.

Wu, W.; Owino, J.; Al-Ostaz, A.; Cai, L. (2014): Applying periodic boundary conditions in finite element analysis. *SIMULIA Community Conference*. https://40.85.176.82/faculty/weidong-wu/pdfs/pbc.pdf.